T. Magn. Soc. Jpn. (Special Issues)., **2**, 37-42 (2018)

<Paper>

# Examination of High-Efficiency Rare Earth Free Motor with Three-Dimensional Magnet Arrangement

H. Saito, Y. Yoshida*, and K. Tajima

Department of Cooperative Major in Life Cycle Design Engineering, Akita Univ., *1-1, Tegata Gakuen-machi, Akita 010-5802, Japan*

*Department of Electrical and Electronic Engineering, Akita Univ., *1-1, Tegata Gakuen-machi, Akita 010-5802, Japan*

In this paper, a high-torque and high-efficiency ferrite magnet motor is presented whose rotor has a three-dimensional (3D) magnet arrangement. First, the rotor structure with 3D magnet arrangement for improving motor torque is described. Next, the effect of toroidal-winding which can improve the winding space factor to reduce copper loss, is discussed. Then, a comparison of efficiency between the proposed motor and conventional surface permanent magnet (SPM) motor with distributed-winding shows an improvement in motor efficiency in a wide operating range.

**Key words:** permanent magnet motor, ferrite magnet, three-dimensional magnet arrangement, toroidal-winding

## 1. Introduction

Electric motors are used for various applications, such as industrial machinery, and electrical equipment, automobiles. Currently, motors occupy about 57.3 % of the domestic electricity consumption in Japan[1]. Among the motors, permanent magnet (PM) motors using rare earth magnets are used for various applications, such as motors for driving Electric vehicles (EVs) and Hybrid electric vehicles (HEVs) due to their high performance characteristics[2]. However, although rare earth magnets whose raw material is based on neodymium and dysprosium are key element for improving the performance of PM motors, they may be subject to rapid price fluctuation as the production of such metals is concentrated in a single country. Therefore, it is important to develop a high-efficiency motor without using rare-earth magnets.

At present, studies are being conducted on rare earth free motors using only ferrite magnets that can be inexpensively and stably supplied as an alternative to rare earth magnets[3),4),5)] as well as on rare earth-less motors in which the usage of rare earth magnets is reduced by using both rare earth magnets and ferrite magnets[6),7)]. The ferrite magnet has about one-third of the residual magnetic flux density and coercive force of the neodymium sintered magnet, which is a rare earth magnet. Therefore, simply replacing the magnet does not produce a magnetic flux equivalent to that of rare earth magnets; thus, the performance of the motors deteriorates[3)].

In this paper, we investigate an increase in torque with a rotor structure having a three-dimensional magnet arrangement for increasing the surface area of the magnet. Furthermore, by adopting toroidal winding as a stator winding method, copper loss is reduced and the efficiency of the motor is improved.

## 2. Torque increase with three-dimensional magnet arrangement

Figure 1 shows a sectional view of a distributed-winding surface permanent magnet (SPM) motor to be compared. Table 1 lists the specifications of the motor.

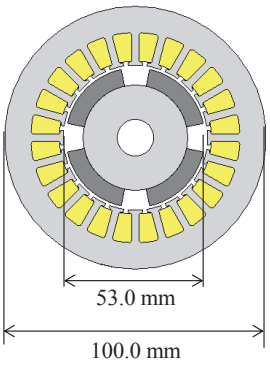


**Fig. 1** Shape of distributed-winding SPM motor.

**Table 1** Specifications of distributed-winding SPM motor.

| Parameters | Value |
|---|---|
| Stator outer diameter (mm) | 100 |
| Rotor outer diameter (mm) | 53 |
| Gap width (mm) | 1.1 |
| Stack length (mm) | 30 |
| Permanent magnet | Ferrite magnet (SSR-420) |
| Core material | 50JN1300 |
| Number of winding turns/slot (turns) | 40 |
| Winding diameter (mm) | $\phi$0.5 |
| Number of slots | 24 |
| Number of poles | 4 |

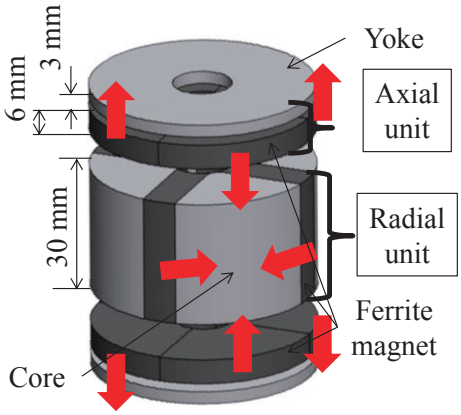


(a) Over view of rotor

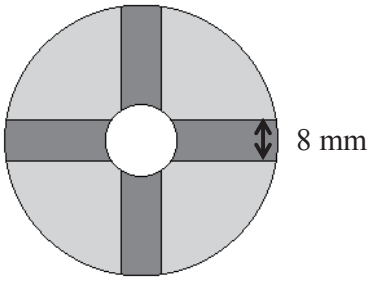


(b) Radial unit

**Fig. 2** Shape of three-dimensional magnet arrangement (3D-MA) model.

To design the three-dimensional magnet arrangement (3D-MA) rotor, three-dimensional finite element analysis (3D-FEA) was performed by using the JMAG-Designer Ver 16.0 software. As ferrite magnets with low coercive force are used for the magnets, demagnetization of the magnets was considered in the analysis.

Figure 2 shows a general view of a three-dimensional magnet arrangement (3D-MA) model. To estimate the effect of the 3D-MA rotor compared with the SPM motor with distributed-winding, the torque of the 3D-MA motor was calculated by using the same stator as the SPM motor shown in Fig. 1. We focused on generating a larger torque with a motor using ferrite magnets. For that purpose, it is necessary to increase the surface area of the magnet[5]. The radial unit adopts a spoke structure to increase the surface area. Although the torque increases as the magnet thickness increases, the magnet thickness was set to 8 mm to secure the contact area between the motor shaft and the rotor core. To further increase the surface area of the magnet, the area in the axial direction is utilized with 3D-MA.

In the model of the proposed 3D-MA, the axial unit is composed of a yoke and four poles of ferrite magnet arranged in the axial direction of the rotor. The axial unit is accommodated within the dead space at the coil end.

Figure 3 shows the relationship between the yoke thickness and the average torque when the thickness of the magnet in the axial direction was 6 mm. If the yoke thickness was larger than 3 mm, the torque did not increase as the yoke thickness increases. The yoke thickness was set to 3 mm, since approximately the same results were obtained with other magnet thicknesses.

Figure 4 shows the relationship between the magnet thickness and the average torque when the yoke thickness was 3 mm. When the magnet in the axial direction was thinner than an air gap length of 1.1 mm, the magnetic flux short-circuited through the axial direction yoke. If the magnet thickness was larger than 2 mm, the torque increased compared with that of the SPM motor. From these characteristics, a magnet thickness of 6 mm was used because the torque was saturated over 6mm.

Table 2 shows a comparison of the magnet surface area of the SPM motor and 3D-MA model. The surface area of the 3D-MA was 110.5% larger than that of the SPM motor.

Figure 5 shows a comparison of the average torque of the SPM motor and 3D-MA model. The average torque of the 3D-MA model was 79% larger than that of the SPM motor.

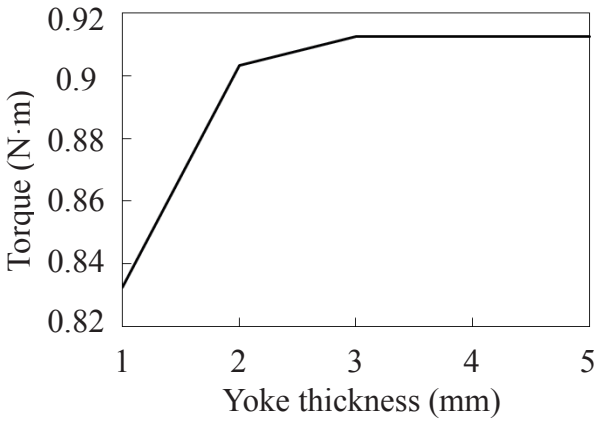


**Fig. 3** Relationship between yoke thickness of axial unit and average torque.

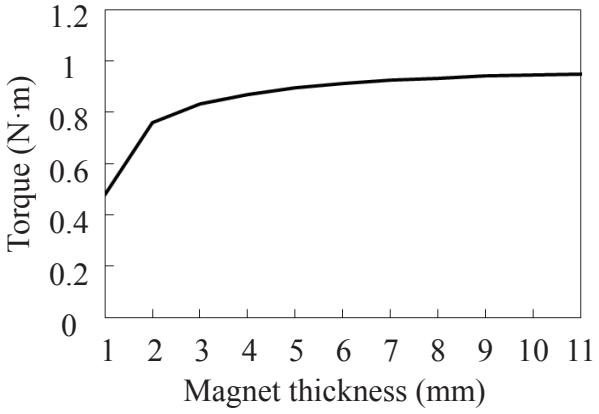


**Fig. 4** Relationship between magnet thickness of axial unit and average torque.

**Table 2** Comparison of surface area.

| | SPM | IPM | 3D-MA |
|---|---|---|---|
| Magnet surface area/pole ($mm^2$) | 919.9 | 1227.1 (+33.4%) | 1936.4 (+110.5%) |

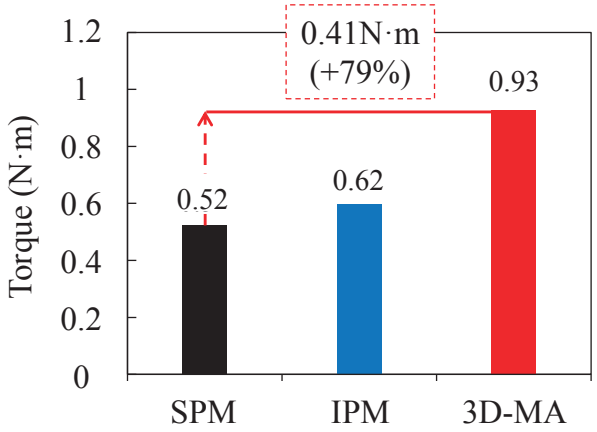


**Fig. 5** Comparison of average torque at current amplitude of 4.0 A.

### 3. Reducing copper loss with toroidal-winding

Figures 6 (a) and (b) show the shape of stators with toroidal-winding and with distributed-winding. The inner and the outer diameters of both winding types are 55.2 and 100 mm, respectively. The coils for toroidal-winding are wound around the back yoke. The outer diameter of the toroidal-winding stator including the coil is designed to have the same outer diameter as the distributed-winding stator.

Figures 7 (a) and (b) show the direction of the current flowing in the coils and a magnetic flux diagram of distributed-winding and toroidal-winding. To compare only the spatial distribution of the magnetomotive force generated by the excitation current between distributed-winding and toroidal-winding, iron cores instead of the magnets were used for the rotors. Figure 8 shows a comparison of the magnetic flux density distribution of the air gap. In the figure, it can be seen that the flux densities generated by both winding methods were almost equal.

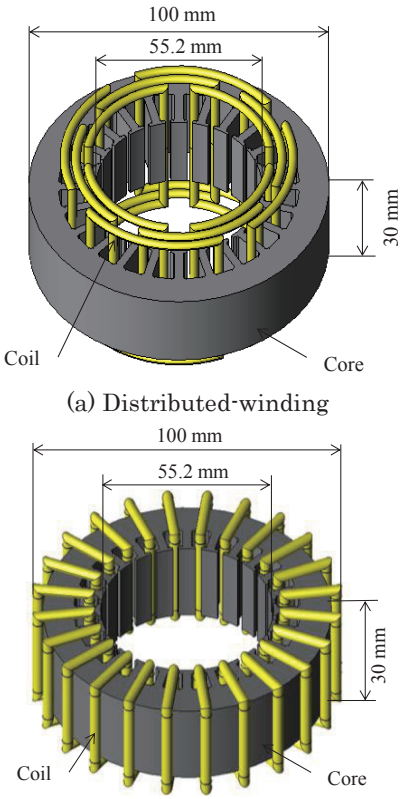


**Fig. 6** Shape of stator with distributed-winding and toroidal-winding.

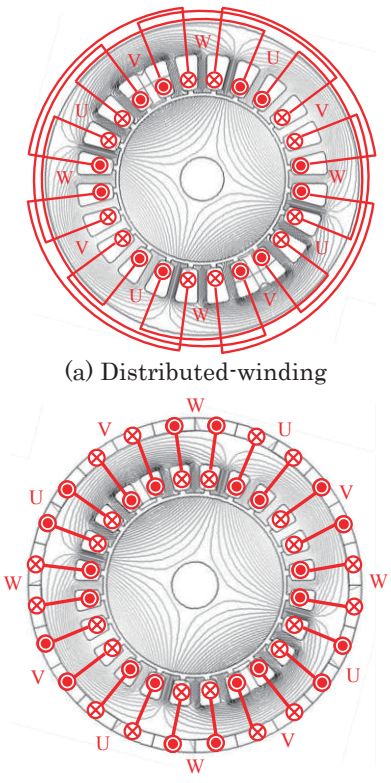


**Fig. 7** Magnetic flux diagram obtained by excitation current.

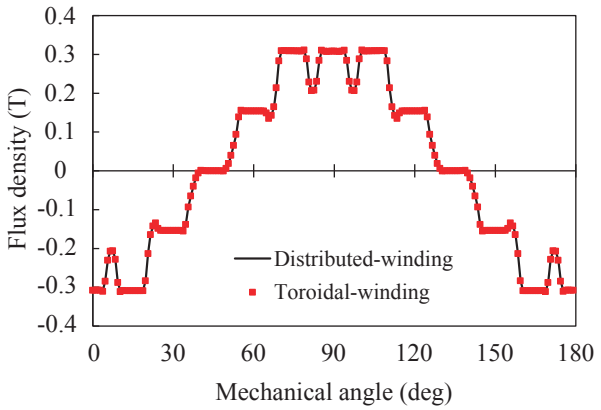


**Fig. 8** Comparison of air-gap flux density distribution with excitation current.

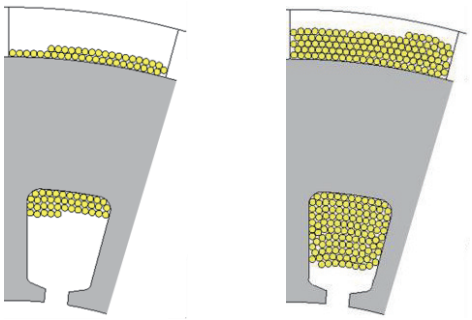

| Number of turns | 40 turns | 120 turns |
|---|---|---|
| Winding space factor | 17% | 50% |

**Fig. 9** Increase in winding factor of toroidal-winding.

Figure 9 shows a comparison of the number of turns and the space factor per one slot of the stator of the toroidal-winding motor used in this study. Since the coil wound in the slot does not interfere with other coils, the number of winding turns of the coil can be increased from 40 turns to 120 turns; the space factor increases from 17% to 50%.

Figure 10 shows a comparison of the torque wave forms of the distributed-winding motor and toroidal-winding motor using the same rotor (SPM rotor). The torque wave form of the toroidal-winding motor was exactly the same as that for the distributed-winding motor.

Figure 11 (a) shows a comparison of the copper loss of each motor at an output of 109 W and a rotation speed of 1000 rpm. The copper loss could be reduced by 44.3 W (65%) by using toroidal-winding compared with distributed-winding. As mentioned in section 2, using the 3D-MA rotor, the excitation current could be suppressed to 2.27 A to produce the same torque as that of the SPM rotor. Therefore, the copper loss at the same output was reduced to 7.5 W. Figure 11 (b) shows a comparison of the iron loss of each motor under the same output conditions at each rotational speed. The iron losses of the proposed 3D-MA motor were more than twice as large as those of the conventional SPM motor. Therefore, the efficiency of the 3D-MA motor worsened in the high-speed rotation region. Because nonconductive ferrite magnets are used for the motors, the eddy current losses in the magnets were not considered.

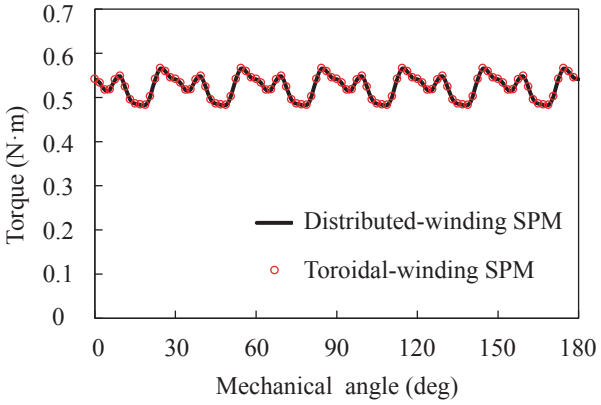


**Fig. 10** Comparison of torque wave form at current amplitude of 4.0 A.

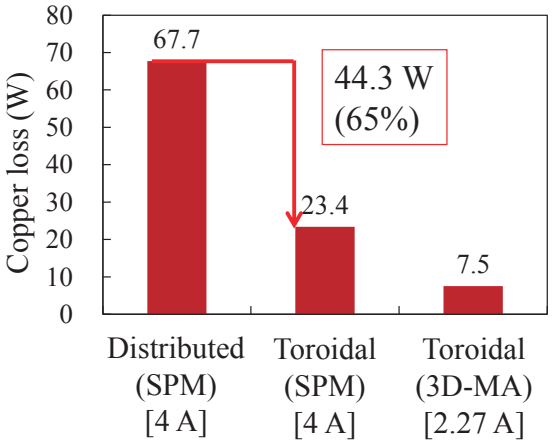


(a) Comparison of copper loss
(output: 109 W, speed: 1000 rpm)

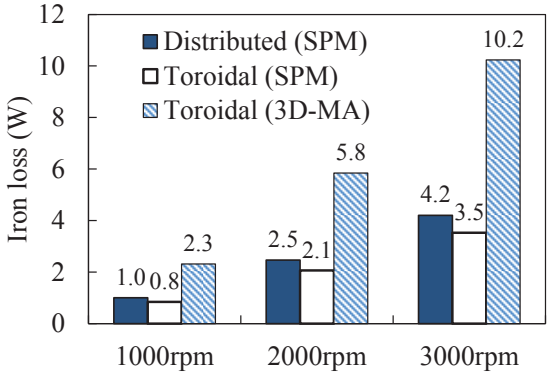


(b) Comparison of iron loss

**Fig. 11** Comparison of loss.

## 4. Comparison of efficiency

In this section, the motor performance is evaluated by using efficiency maps. The maximum line voltage and the maximum phase current amplitude are 48 V and 4 A to calculate the efficiency. The efficiency, $\eta$, is calculated by

$$\eta = \frac{\omega T}{\omega T + W_i + W_c} \cdots\cdots (1)$$

where $\omega$, $T$, $W_i$, and $W_c$ are the angular velocity, torque, iron loss and copper loss obtained by analysis and calculation.

Figure 12 shows the result of calculating efficiency for each motor.

By comparing (a) and (b) in Fig. 12, the effect of copper loss reduction with toroidal-winding can be seen. Figure 13 shows the difference in motor efficiency obtained by subtracting the efficiency of the SPM motor with distributed-winding from the efficiency of that with toroidal-winding. Although the output ranges of the distributed-winding SPM motor and toroidal-winding SPM motor completely coincided with each other, the efficiency of the toroidal-winding SPM motor was improved throughout the entire out range by reducing the copper loss.

As can be seen by comparing (b) and (c) in Fig. 12, the maximum torque of 3D-MA motor was increased by 79% by increasing the magnet surface area. However, since the reactive magnetomotive force at a high rotational speed increased, the maximum rotational speed decreased compared with the SPM motor. Figure 14 shows the difference in motor efficiency obtained by subtracting the efficiency of the SPM motor with toroidal-winding from that of the 3D-MA motor. When comparing the efficiency in the same output range, the efficiency of the 3D-MA model was higher than that of the SPM motor in a wide range except the high rotation speed and low torque region.

## 5. Conclusion

In this paper, we examined a motor that does not contain rare earth metals. First, we proposed a 3D-MA model whose rotor magnets are arranged in three dimensions in order to increase the magnet surface area. As a result, the maximum torque of the 3D-MA motor was increased by 79% compared with the conventional SPM motor. Next, a winding method for reducing copper loss further compared with the conventional distributed-winding was presented. The proposed toroidal-winding can reduce the copper loss by 65% with an increased winding space factor. The combination of a 3D-MA rotor and toroidal-winding stator improved the motor efficiency in a wide range, especially the high-torque region.

As further work, we will determine the effectiveness of the proposed motor by manufacturing an actual machine on an experimental basis.

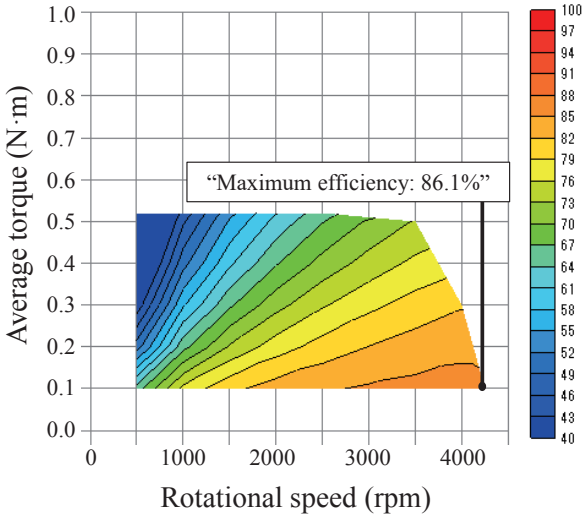


(a) Distributed-winding SPM motor

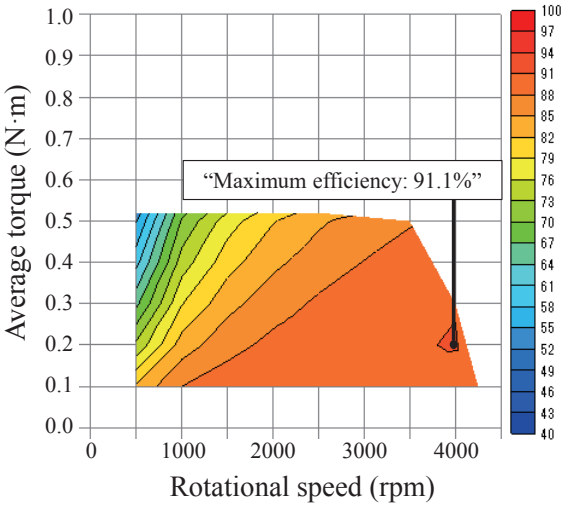


(b) Toroidal-winding SPM motor

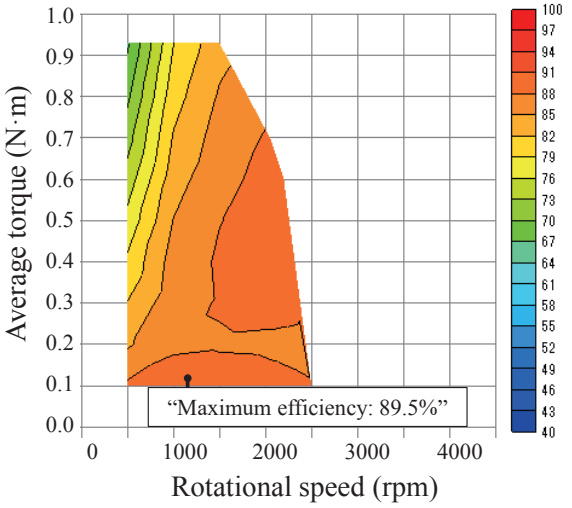


(c) Toroidal-winding 3D-MA

**Fig. 12** Efficiency maps of each motor.

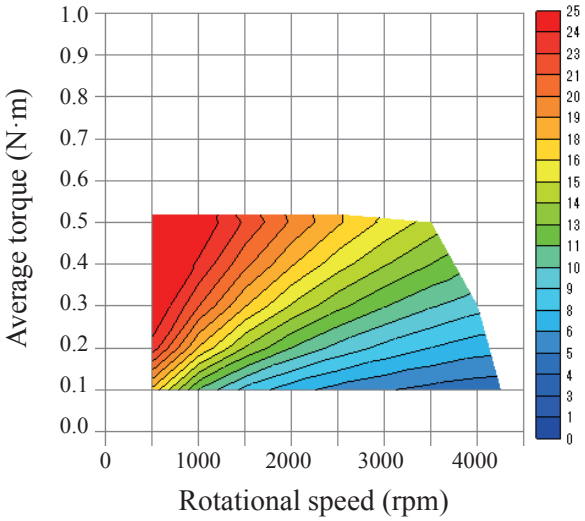


**Fig. 13** Comparison of efficiency between SPM motors with distributed-winding and with toroidal-winding.

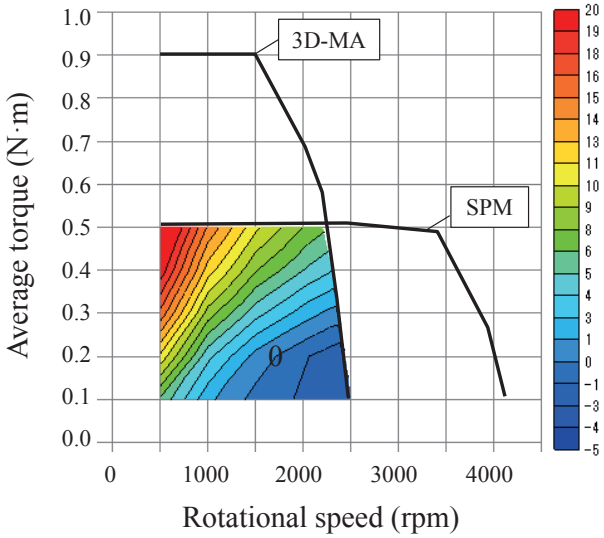


**Fig. 14** Comparison of efficiency between 3D-MA and SPM motor with toroidal-winding.

## References


1) Zaidannhoujinn Sinnkinousosikennkyuukaihatukyoukai: "Dennryokusiyoukiki no Syouhidennryokuryou nikannsuru Gennjou to Kinnmirai no Doukoutyousa" (in Japanese), *Research Report* (2009).
2) M. Obata, S. Morimoto, M. Sanada, and Y.Inoue: "Characteristic of PMASynRM with Ferrite Magnets for EV/HEV Applications," *ICEMS* 2012, DS3G2-7 (2012).
3) Y. Iwai, Y. Yoshida, and K. Tajima: "Consideration of Efficiency Improvement of Ferrite Magnet Motor with Toroidal Winding," *The Papers of Technical Meeting on Magnetics IEEJ*, MAG 15-117 (2015).
4) M. Sanada, Y. Inoue, and S. Morimoto: "Structure and Characteristics of High-Performance PMASynRM with Ferrite Magnets," *IEEJ Trans. IA,* **13**, 1401 (2011).
5) D. Matsuhashi, K. Matsuo, T. Okitsu, and T. Ashikaga: "Comparison Study of Various Motors for EVs and the Potentiality of a Ferrite Magnet Motor," *IEEJ Journal of* IA, **4**, 174 (2014).
6) S. Ishii, Y. Hasegawa, K. Nakamura, and O. Ichinokura: "Novel Flux Barrier type Outer Rotor IPM Motor with Rare-earth and Ferrite Magnets," *J. Magn. Soc. Jpn*, **37**, 259 (2013).
7) W. Wu, X. Zhu, L. Quan, Z. Xiang, D. Fan, and S. Yang : "Performance Evaluation of a U-shaped Less-rare-earth Hybrid Permanent Magnet Assisted Synchronous Reluctance Motor," *IEEE* (2016).



**Received Oct. 13, 2017; Revised Dec.21, 2017; Accepted Feb. 12, 2018**